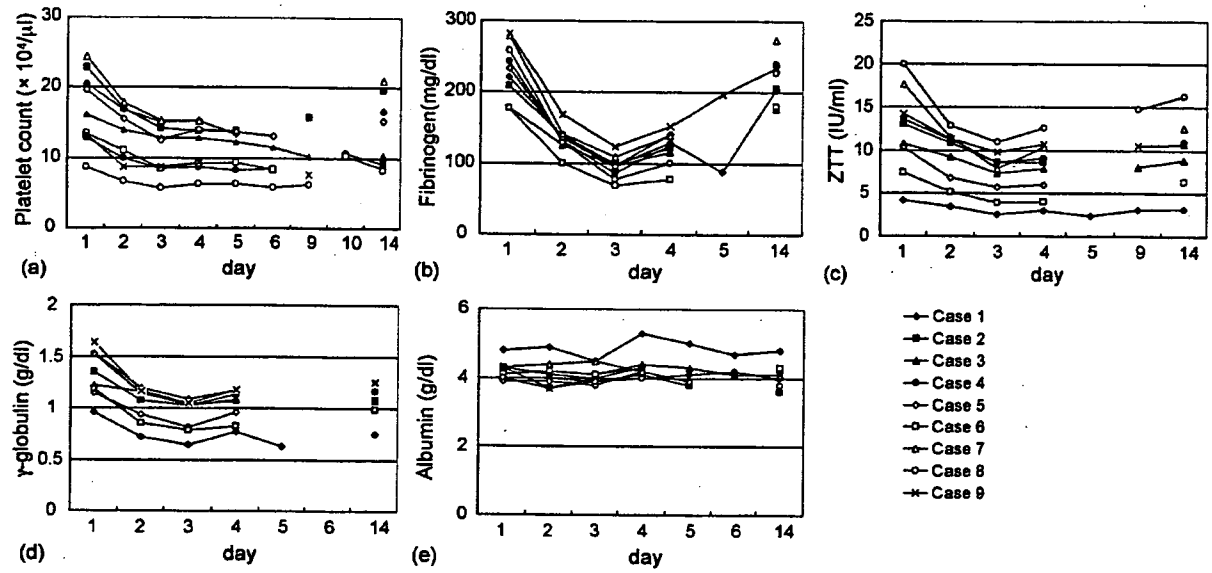

Fig. 5. Changes in the laboratory findings during treatment: (a) platelet count, (b) fibrinogen, (c) ZTT, (d) γ-globulin, and (e) albumin.

and ribavirin combination therapy for 24 weeks, and the other received IFN and ribavirin combination therapy for 24 weeks, followed by additional IFN monotherapy for 24 weeks. These patients were two of the four patients in whom the HCV RNA was quantitatively undetectable after 2 weeks of therapy. Treatment of the other two patients was discontinued before 24 weeks due to adverse events (skin eruption, anorexia, and general malaise). In the six patients for whom complete treatment was possible, the SVR rate was 33.3% (2/6) (a per-protocol approach).

In the control group, the SVR rate was 18. About 2% (2/11) as determined using an intent-to-treat approach and 20.0% (2/10) as determined using a per-protocol approach. The difference in the SVR rate between the two groups was not statistically significant ($P = 0.822$ and 0.551, respectively).

The factors associated with the SVR in our patients were analyzed using uni- and multi-variate analysis. Using univariate analysis, the EVR was found to be the only factor associated with SVR ($P = 0.025$). Associations with other factors, such as DFPP, age, sex, pre-treatment history, and fibrosis, were not detected in our series ($P = 0.822$, 0.170, 0.822, 0.822, and 0.052, respectively). Using multivariate analysis, the association of all of these factors was found to be statistically insignificant.

In the DFPP group, the only factor showing a relationship with the SVR was the viral negativity at 2 weeks ($P = 0.014$).

3.6. Safety and adverse events

In eight of the patients, DFPP was performed three times on days 1, 2, and 4. It was not performed on day 4 in one patient because this patient's fibrinogen level was lower than 100 mg/dl before DFPP; hence, DFPP was performed only twice in this patient.

The changes in laboratory test values as a result of DFPP treatment were also investigated. After DFPP on day 1, the platelet count decreased on average by 22.5%. The decrease persisted until the completion of DFPP and then slowly recovered by 2 weeks after the initiation of the therapy. The fibrinogen level decreased by 30–50% after DFPP on day 1. It decreased to its lowest level on day 3, slowly recovered after the completion of DFPP, and then returned to a level similar to the pre-DFPP level by 2 weeks after the initiation of the therapy. The ZTT values and the γ-globulin and total cholesterol levels also showed similar changes. No change was observed in the serum albumin level (Fig. 5).

The adverse events that occurred during the IFN and DFPP combination therapy are listed in Table 2. Most of these were influenza-like symptoms and digestive symptoms that were associated with the IFN and ribavirin combination therapy. The adverse events attributable to concomitant DFPP and IFN therapy were mild hypotension in two patients and mild

Table 2
Rates of discontinuation of treatment, dose reduction, and occurrence of adverse events during treatment

Adverse events	*n* (%)
Influenza-like symptoms	8 (89)
Skin eruption	1 (11)
Gastrointestinal symptoms	6 (67)
Insomnia	2 (22)
Hypotension	2 (22)
Vagal reflux	1 (11)
Depression	5 (56)
Anemia	7 (78)
Neutropenia	1 (11)
Thrombocytopenia	1 (11)
Dose reduction	4 (44)
Discontinuation of treatment	3 (33)

transient vagal reflex in one patient. These events occurred during DFPP, and fluid drip injection resulted in rapid recovery from these symptoms. A blood test revealed decreases in the hemoglobin as well as in the neutrophil and platelet counts; however, these were observed during IFN therapy, suggesting that they were unrelated to the DFPP. The ribavirin dose was reduced in three patients due to anorexia, anemia, and skin eruption. The IFN dose was reduced in one patient due to neutropenia. It was difficult to continue the IFN and ribavirin combination therapy in three patients due to skin eruption, anorexia, and systemic malaise; therefore, in these patients the therapy was discontinued.

4. Discussion

Currently, the most promising therapy for chronic hepatitis C is a 48-week PEG-IFN and ribavirin combination therapy. Using this approach, the SVR is increased in approximately 50% of patients [20]. However, in the other half, HCV viremia persists and, although ALT is stabilized, hepatitis activity may again increase several years later. Alternatively, chronic hepatitis persists without the normalization of ALT and may progress to liver cirrhosis resulting in hepatocellular carcinoma. To prevent these events from occurring, it is necessary to develop other novel ideas or novel drugs for therapy. With regard to ideas for therapy, long-term IFN therapy extended over 48 weeks, the use of intravenously administrable IFN-β, and concomitant IFN and high-dose ribavirin therapy with simultaneous monitoring of the blood ribavirin concentration, have been investigated [21]. With regard to novel drugs, amantadine, IL-12, and thymosin-α1 are concomitantly used with IFN therapy or with IFN and ribavirin combination therapy [22–24]. With regard to novel antiviral agents, the development of an antisense complex targeting the viral IRES, a serine protease inhibitor targeting NS3 protease, and a polymerase inhibitor targeting NS5B have been investigated [8–11].

Previous reports have described the various factors that affect the SVR produced by IFN therapy for chronic hepatitis. The patient-related factors include gender, age, the presence or absence of concomitant ribavirin treatment, and the stage of liver fibrosis; the viral factors include the viral genotype, HCV RNA level before therapy, and the number of mutations in the NS5A interferon sensitivity-determining region (ISDR) of genotype 1b [25]. Recently, an EVR has been recognized as an important factor for achieving an SVR using IFN therapy. An EVR is defined as virus elimination at an early stage after the initiation of treatment. An EVR in 2 weeks with IFN monotherapy and 12 weeks with IFNα-2b and ribavirin combination therapy has been shown to be frequent in SVR cases, and the probability of achieving an SVR is high when the virus is eliminated from the circulation within these early stages [12,13].

In this study, we focused on the HCV RNA level before therapy and attempted to reduce the viral load of chronic genotype 1b hepatitis C patients, with a high viral load of 100 KIU/ml or higher, by performing plasmapheresis therapy, DFPP, before the initiation of IFN therapy. Thus far, this is the first attempt to study the efficacy of a combination of IFN therapy and plasmapheresis with chronic hepatitis C patients.

In previous studies, Manzin et al. measured the HCV RNA in chronic hepatitis C patients with cryoglobulinemia before and after plasma exchange; they found that the HCV RNA was reduced by 45.3–93.3% after treatment but returned to its previous level after 4–6 h [14]. Similarly, Ramratnam et al. observed a decrease in the viral load after plasmapheresis in HIV-1- and HCV-positive patients [26]. It has also been reported that heparin-induced extracorporeal low-density lipoprotein (LDL) precipitation (HELP) apheresis decreased the HCV RNA in chronic hepatitis C patients with the complication of hypercholesterolemia [16,17,27]. The decrease in the HCV RNA was transient according to these reports. By fitting a mathematical model to the changes in viral load during IFN therapy, HCV production in the liver has been estimated to be 10^{12} particles per day [28]. Although the virus is eliminated from the blood, virus production continues in the liver unless it is inhibited by IFN; hence, the HCV RNA level may return to the pre-therapy level after a few hours. Therefore, we planned to administer IFN immediately after the first plasmapheresis.

We selected DFPP as a plasmapheresis technique because there was no necessity to exchange plasma and supplement albumin during the apheresis.

Since DFPP is based on the principle of size separation, the membrane with a mean pore size of 30 nm that was used as the second filter in this study can theoretically be expected to eliminate HCV particles with a diameter of 55–65 nm. After the DFPP second filtration, the HCV RNA was quantitatively undetectable after performing DFPP for 1 and 3 h; this implies that the filter could eliminate HCV particles and that the efficiency did not change with time.

Other low molecular weight substances, including albumin (MW 66 kDa) and ribavirin (MW 244 kDa), passed through the second membrane and were returned to patient's blood. Hence, low molecular weight substances were not eliminated by this DFPP system.

In seven patients, in whom the serum HCV RNA level could be measured before and after DFPP on day 1, the mean rate at which the HCV RNA level decreased was 48% (18–78%); the HCV RNA level did not increase again. This exclusion may have been due to the inhibition of virus production by the IFN therapy that was initiated immediately after DFPP.

The EVR after 2 weeks of therapy tended to be higher in the DFPP group than in the control group. The change in viral load after 2 weeks also tended to decrease more in the DFPP group than in the control group. However, both these differences were statistically insignificant. The virus negativity in the DFPP group after 4 and 8 weeks was 66.7% and 62.5%, respectively. In the control group, the HCV RNA levels were not measured periodically and therefore no comparison was

possible. However, in a double-blind, controlled study in Japan on IFNα-2b and ribavirin combination therapy for chronic genotype 1b hepatitis C patients with a high viral load, Iino et al. found that the HCV RNA negativity after 4 and 8 weeks after the initiation of therapy was 18.8% and 38.2%, respectively. This suggested that IFN therapy with a concomitant reduction of the viral load using DFPP may induce an early conversion to the HCV RNA-negative state.

In our study, an SVR was observed in 2 of the 9 patients (22.2%) in the DFPP group and in 2 of the 11 patients (18.2%) in the control group. These rates are comparable to the result in which an SVR was observed in 19.0% of chronic genotype 1b HCV patients after 24 weeks after the administration of an interferon and ribavirin combination therapy [30]. An SVR observed in DFPP group was not higher than that in control group although an EVR on 2 weeks in DFPP was relatively higher than that in control group. One of the possible reasons for this observation is that, in two of the six patients exhibiting an EVR, treatment was discontinued because of the adverse events. EVR was demonstrated to be the only factor related to SVR by univariate analysis in our study; this may have been because the number of patients was insufficient to conduct an accurate analysis of these factors.

With regard to the safety of the IFN and ribavirin combination therapy with concomitant DFPP, only mild hypotension and transient vagal reflex were observed after the initiation of DFPP, and these were rapidly resolved. There were no other adverse events attributable to concomitant DFPP, and the treatment was performed safely. Since DFPP is frequently used in the treatment of severe disease conditions, such as malignant rheumatoid arthritis, thrombotic thrombopenic purpura, and multiple sclerosis, there may be no problems with the application of this procedure to chronic hepatitis patients. During the treatment, a catheter was inserted in the right femoral vein for DFPP; however, no infection or accident occurred as a consequence of its indwelling. The other adverse events were attributable to the ribavirin and IFN therapy.

With regard to results of the blood test, the platelet count and fibrinogen level slowly decreased from the initiation of therapy until the completion of DFPP; however, these gradually recovered after the completion of DFPP. On day 3, the fibrinogen level was lower than 100 mg/dl in all but two patients. To ensure the safety of the patients, and to prevent complications such as hemorrhage, DFPP conducted three times on days 1, 2, and 4 during the first week of therapy may be appropriate for patients with chronic hepatitis C.

In view of the fact that we found no significant difference in the EVR and SVR between the DFPP and control groups, and because the number of patients was very small, it was not possible in this preliminary study to draw conclusions regarding the applicability of the DFPP used in conjunction with ribavirin and IFN therapy. It could be argued that a simple physical reduction in the viral load, induced by concomitant DFPP or other apheresis, is really significant for the ribavirin and IFN therapy for chronic hepatitis C patients with a high viral load. Based on our results, it may be possible to use DFPP to facilitate early viral elimination. However, the early viral elimination by DFPP was not related to an SVR. Although five of the eight patients (62.5%, therapy was discontinued in one patient after 7 weeks) became virus-negative after 8 weeks, an SVR was observed in only two patients; thus, the relationship between the early virus negativity obtained by DFPP and the SVR remains unclear. Since the early conversion to the virus-negative state is a result of the reactivity of the host and virus to ribavirin and IFN, it may be possible that a simple physical reduction in the amount of the virus is not significant. However, DFPP eliminates not only the virus but also macromolecules including immunoglobulins. The elimination of some humoral factors or complement components by the dialysis membrane might be involved. The state of HCV in the blood, such as the immunoglobulin-bound state, the lipoprotein-associated state, and the non-bound (free) state, may also be important. In two preliminary cases, the state of HCV during the treatment was investigated using differential flotation centrifugation. In differential floatation centrifugation, the hyperbaric fraction, including the immunoglobulin-bound HCV particles, settles to the bottom, whereas the hypobaric fraction, including free-state HCV particles, rises to the top. In the two examined cases, the bottom: top ratio was reduced after the first DFPP treatment; from 214 to 62 in case 1 and from 108 to 46 in case 2. Since a decline in the bottom: top ratio indicates an increased amount of free-state HCV particles compared to the amount of immunoglobulin-bound HCV particles, these results suggest that the occurrence of the free-state HCV increased after DFPP. This increase in the amount of free-state HCV may possibly involve an SVR; this supposition is based on a previous study that demonstrated that a high proportion of free-state HCV was related to an SVR [29].

In conclusion, in order to achieve a reduction in the level of HCV RNA before IFN therapy and to facilitate an early conversion to a virus-negative state, plasmapheresis therapy (DFPP) was performed on chronic genotype 1b hepatitis C patients with a high viral load. The therapy was performed without the occurrence of severe adverse events, and the results suggested the possibility that concomitant DFPP increased the rate of early conversion to a virus-negative state. Since only nine patients were treated and IFN administration was discontinued in three patients, the relationship between DFPP and an EVR or SVR is unclear. If an EVR is achieved by a combination of DFPP and interferon therapy, and this is related to an SVR, the combination therapy with DFPP will not only be of benefit to chronic hepatitis C patients with a high viral load but may also shorten the period of interferon therapy. Furthermore, the cost of interferon therapy will also be reduced, although the cost of performing DFPP three times will remain high at approximately 2500 dollars. Because our study was limited by the small number of patients, further investigations using a study design that clarifies the relationship between DFPP and an EVR or SVR are necessary. It is also important to further investigate the

antiviral effect of the PEG-IFN and ribavirin combination therapy with concomitant DFPP, and the effects of DFPP other than virus elimination. In order to clarify this relationship, a multi-center clinical trial is being undertaken in Japan, and the data from this study is currently being collected.

Acknowledgements

This study was supported by Asahi Kasei Medical Co. Ltd. (Tokyo, Japan). We thank Satoshi Saikawa, Hidetomo Takeuchi, and Tomoko Ino for providing technical support.

References

[1] Yoshida H, Shiratori Y, Moriyama M, et al. Interferon therapy reduces the risk for hepatocellular carcinoma: national surveillance program of cirrhotic and noncirrhotic patients with chronic hepatitis C in Japan. IHIT Study Group. Inhibition of hepatocarcinogenesis by interferon therapy. Ann Intern Med 1999;131:174–81.

[2] McHutchison JG, Gordon SC, Schiff ER, et al. Interferon alfa-2b alone or in combination with ribavirin as initial treatment for chronic hepatitis C. Hepatitis Interventional Therapy Group. N Engl J Med 1998;339:1485–92.

[3] Iino S, Matsushima T, Kumada H, Kiyosawa K, Kakumu S, Hayashi Y. Comparison of ribavirin (SCH18908) and interferon α-2b combination therapy and interferon α-2b monotherapy in chronic hepatitis C patients of genotype 1b and high viral load—a double blind parallel study to determine dosage and administration. Rinsyou Iyaku (J Clin Therap Med) 2002;18:565–91.

[4] Poynard T, Marcellin P, Lee SS, et al. Randomised trial of interferon alpha 2b plus ribavirin for 48 weeks or for 24 weeks versus interferon alpha 2b plus placebo for 48 weeks for treatment of chronic infection with hepatitis C virus. International Hepatitis Interventional Therapy Group (IHIT). Lancet 1998;352:1426–32.

[5] Poynard T, McHutchison J, Goodman Z, Ling MH, Albrecht J. Is an "a la carte" combination interferon alfa-2b plus ribavirin regimen possible for the first line treatment in patients with chronic hepatitis C? The ALGOVIRC Project Group. Hepatology 2000;31:211–8.

[6] Fried MW, Shiffman ML, Reddy KR, et al. Peginterferon alfa-2a plus ribavirin for chronic hepatitis C virus infection. N Engl J Med 2002;347:975–82.

[7] Iino SOK, Omata M, Kumada H, Hayashi N, Tanikawa K. Clinical efficacy of PEG-interferon α-2b and ribavirin combination with interferon α-2b and ribavirin combination therapy for 24 weeks. KAN TAN SUI 2004;49:1099–121 [in Japanese].

[8] Lamarre D, Anderson PC, Bailey M, et al. An NS3 protease inhibitor with antiviral effects in humans infected with hepatitis C virus. Nature 2003;426:186–9.

[9] Love RA, Parge HE, Yu X, et al. Crystallographic identification of a noncompetitive inhibitor binding site on the hepatitis C virus NS5B RNA polymerase enzyme. J Virol 2003;77:7575–81.

[10] Soler M, McHutchison JG, Kwoh TJ, Dorr FA, Pawlotsky JM. Virological effects of ISIS 14803, an antisense oligonucleotide inhibitor of hepatitis C virus (HCV) internal ribosome entry site (IRES), on HCV IRES in chronic hepatitis C patients and examination of the potential role of primary and secondary HCV resistance in the outcome of treatment. Antivir Ther 2004;9:953–68.

[11] Pudi R, Ramamurthy SS, Das S. A peptide derived from RNA recognition motif 2 of human 1a protein binds to hepatitis C virus internal ribosome entry site, prevents ribosomal assembly, and inhibits internal initiation of translation. J Virol 2005;79:9842–53.

[12] Davis GL. Monitoring of viral levels during therapy of hepatitis C. Hepatology 2002;36:S145–51.

[13] Davis GL, Wong JB, McHutchison JG, Manns MP, Harvey J, Albrecht J. Early virologic response to treatment with peginterferon alfa-2b plus ribavirin in patients with chronic hepatitis C. Hepatology 2003;38:645–52.

[14] Manzin A, Candela M, Solforosi L, Gabrielli A, Clementi M. Dynamics of hepatitis C viremia after plasma exchange. J Hepatol 1999;31:389–93.

[15] Fabrizi F, Martin P, Dixit V, et al. Biological dynamics of viral load in hemodialysis patients with hepatitis C virus. Am J Kidney Dis 2000;35:122–9.

[16] Schettler V, Monazahian M, Wieland E, et al. Reduction of hepatitis C virus load by H.E. L. P.-LDL apheresis. Eur J Clin Invest 2001;31:154–5.

[17] Schettler V, Monazahian M, Wieland E, Thomssen R, Müller GA. Effect of heparin-induced extracorporeal low-density lipoprotein precipitation (HELP) apheresis on hepatitis C plasma virus load. Ther Apher 2001;5:384–6.

[18] Kaito M, Watanabe S, Tsukiyama-Kohara K, et al. Hepatitis C virus particle detected by immunoelectron microscopic study. J Gen Virol 1994;75:1755–60.

[19] Ichida F. New Inuyama classification: new criteria for histological assessment of chronic hepatitis. Int Hepatol Commun 1996;6:112.

[20] Saracco G, Olivero A, Ciancio A, Carenzi S, Rizzetto M. Therapy of chronic hepatitis C: a critical review. Curr Drug Targets Infect Disord 2003;3:25–32.

[21] Lindahl K, Stahle L, Bruchfeld A, Schvarcz R. High-dose ribavirin in combination with standard dose peginterferon for treatment of patients with chronic hepatitis C. Hepatology 2005;41:275–9.

[22] Abbas Z, Hamid SS, Tabassum S, Jafri W. Thymosin alpha 1 in combination with interferon alpha and ribavirin in chronic hepatitis C patients who are non-responders or relapsers to interferon alpha plus ribavirin. J Pak Med Assoc 2004;54:571–4.

[23] Poo JL, Sanchez-Avila F, Kershenobich D, Garcia-Samper X, Gongora J, Uribe M. Triple combination of thymalfasin, peginterferon alfa-2a and ribavirin in patients with chronic hepatitis C who have failed prior interferon and ribavirin treatment: 24-week interim results of a pilot study. J Gastroenterol Hepatol 2004;19:S79–81.

[24] Kullavanuaya P, Treeprasertsuk S, Thong-Ngam D, Chaermthai K, Gonlachanvit S, Suwanagool P. The combined treatment of interferon alpha-2a and thymosin alpha 1 for chronic hepatitis C: the 48 weeks end of treatment results. J Med Assoc Thai 2001;84(Suppl 1):S462–8.

[25] Pascu M, Martus P, Hohne M, et al. Sustained virological response in hepatitis C virus type 1b infected patients is predicted by the number of mutations within the NS5A-ISDR: a meta-analysis focused on geographical differences. Gut 2004;53:1345–51.

[26] Ramratnam B, Bonhoeffer S, Binley J, et al. Rapid production and clearance of HIV-1 and hepatitis C virus assessed by large volume plasma apheresis. Lancet 1999;354:1782–5.

[27] Marson P, Boschetto R, De Silvestro G, et al. Changes in HCV viremia following LDL apheresis in a HCV positive patient with familial hypercholesterolemia. Int J Artif Organs 1999;22:640–4.

[28] Neumann AU, Lam NP, Dahari H, et al. Hepatitis C viral dynamics in vivo and the antiviral efficacy of interferon-alpha therapy. Science 1998;282:103–7.

[29] Sakai A, Kaneko S, Matsushita E, Kobayashi K. Floating density of hepatitis C virus particles and response to interferon treatment. J Med Virol 1998;55:12–7.

[30] Nagaki M, Imose M, Naiki T, et al. Prospective study on early virologic response to treatment with interferon alpha-2b plus ribavirin in patients with chronic hepatitis C genotype lb. Hepatol Res 2005;33:285–91.

Different Signaling Pathways in the Livers of Patients With Chronic Hepatitis B or Chronic Hepatitis C

Masao Honda, Taro Yamashita, Teruyuki Ueda, Hajime Takatori, Ryuhei Nishino, and Shuichi Kaneko

The clinical manifestations of chronic hepatitis B (CH-B) and chronic hepatitis C (CH-C) are different. We previously reported differences in the gene expression profiles of liver tissue infected with CH-B or CH-C; however, the signaling pathways underlying each condition have yet to be clarified. Using a newly constructed cDNA microarray consisting of 9614 clones selected from 256,550 tags of hepatic serial analysis of gene expression (SAGE) libraries, we compared the gene expression profiles of liver tissue from 24 CH-B patients with those of 23 CH-C patients. Laser capture microdissection was used to isolate hepatocytes from liver lobules and infiltrating lymphoid cells from the portal area, from 16 patients, for gene expression analysis. Furthermore, the comprehensive gene network was analyzed using SAGE libraries of CH-B and CH-C. Supervised and nonsupervised learning methods revealed that gene expression was correlated more with the infecting virus than any other clinical parameters such as histological stage and disease activity. Pro-apoptotic and DNA repair responses were predominant in CH-B with p53 and 14-3-3 interacting genes having an important role. In contrast, inflammatory and anti-apoptotic phenotypes were predominant in CH-C. These differences would evoke different oncogenic factors in CH-B and CH-C. In conclusion, we describe the different signaling pathways induced in the livers of patients with CH-B or CH-C. The results might be useful in guiding therapeutic strategies to prevent the development of hepatocellular carcinoma in cases of CH-B and CH-C. ***Supplementary material for this article can be found on the HEPATOLOGY website (http://interscience.wiley.com/jpages/0270-9139/suppmat/index.html).*** **(HEPATOLOGY 2006;44:1122-1138.)**

The human liver infected with hepatitis B virus (HBV) and hepatitis C virus (HCV) develops chronic hepatitis, cirrhosis, and in some instances, hepatocellular carcinoma (HCC).[1-3] The virological features of these 2 viruses are completely different. HBV is a DNA virus that integrates into the host genome.[4,5] HBV proteins, which have been reported to have transcriptional transactivator activity, may be related to the occurrence of HCC.[6-9] By contrast, HCV is a positive stranded RNA virus that replicates in the cytoplasm.[2] There are some reports that HCV proteins localize to the nucleus or interact with nuclear proteins.[10,11] Nevertheless, both viruses infect the liver and cause chronic hepatitis, which is not distinguishable by histological examination or clinical manifestations.[12] In chronic viral hepatitis, increased numbers of immunoregulatory cells infiltrate the liver, but the functional relevance of these cells to the pathogenesis of chronic hepatitis is not known.

We previously reported that the gene expression profiles in the livers of patients with chronic hepatitis B (CH-B) or chronic hepatitis C (CH-C) are different, and revealed some characteristic features of each disease.[13] However, the independent expression profiles of infiltrated lymphocytes and hepatocytes have yet to be clarified, as do the detailed signaling pathways underlying these 2 conditions.

In this study, we investigated the signaling pathways underlying CH-B and CH-C using cDNA microarray and serial analysis of gene expression (SAGE) techniques. Using laser capture microdissection (LCM), we selectively isolated hepatocytes from liver lobules and infiltrat-

Abbreviations: CH-B, chronic hepatitis B; CH-C, chronic hepatitis C; SAGE, serial analysis of gene expression; HBV, hepatitis B virus; HCV, hepatitis C virus; HCC, hepatocellular carcinoma; GO, gene ontology; LCM, laser capture microdissection; ALT, alanine aminotransferase; aRNA, antisense RNA; CTL, cytotoxic lymphocyte; Cy, cyanine; EGFR, epidermal growth factor receptor; cDNA, complementary DNA; IFN, interferon; NF-κB, nuclear factor-κB; NK cells, natural killer cells.

From the Department of Gastroenterology, Kanazawa University Graduate School of Medicine, Kanazawa, Japan.

Received April 29, 2006; accepted August 8, 2006.

Address reprint requests to: Shuichi Kaneko, M.D., Ph.D., Department of Gastroenterology, Graduate School of Medicine, Kanazawa University, Takara-Machi 13-1, Kanazawa, 920-8641, Japan. E-mail: skaneko@medf.m.kanazawa-u.ac.jp; fax: (81) 76-234-4250.

Published online in Wiley InterScience (www.interscience.wiley.com).

DOI 10.1002/hep.21383

Potential conflict of interest: Nothing to report.

ing lymphoid cells from the portal area, from biopsy specimens, and analyzed their gene expression profiles.

Patients and Methods

Patients. The subjects were 27 patients with CH-B and 26 with CH-C at the Graduate School of Medicine, Kanazawa University Hospital, Japan, between 1999 and 2003 (Table 1). Informed consent was obtained from all patients and ethics approval for the study was obtained from the ethics committee for human genome/gene analysis research at Kanazawa University Graduate School of Medicine. Liver biopsy samples were taken from 24 CH-B patients and 23 CH-C patients, and were divided into 3 portions: one was immersed in formalin for histological assessment, another was immediately frozen in liquid nitrogen for further RNA isolation, and the final portion was frozen in OCT compound for LCM analysis and stored at −80°C until use. Tissue samples from the remaining 6 patients with HCC were surgically obtained from the noncancerous parts of the liver and immediately frozen in liquid nitrogen for SAGE analysis. For normal liver, surgically obtained tissue samples of 6 patients who showed no clinical signs of hepatitis were used, as described.[13]

The grading and staging of chronic hepatitis were histologically assessed according to the method described by Desmet et al.[14] (Table 1). There were no significant differences in the degree of histological activity or staging, nor in the sex or age of patients with CH-B or CH-C (Table 1).

Treatment of Cultured Cells With Interferon-α. Huh-7 cells were treated with recombinant interferon-α (IFN-α) (Schering-Plough Corp., Osaka, Japan) at a concentration of 1000 IU/mL for 6 hours, and were harvested for analysis of induced gene expression by cDNA microarray.

Preparation of cDNA Microarray Slides. In addition to the in-house cDNA microarray slides consisting of 1080 cDNA clones as described,[13,15-19] we made a new cDNA microarray slide for a detailed analysis of the signaling pathways involved in metabolism and enzyme function in liver disease. Besides cDNA microarray analysis, a total of 256,550 tags were obtained from hepatic SAGE libraries (derived from normal liver, CH-C, CH-C related HCC, CH-B, and CH-B related HCC), including 52,149 unique tags. Among these, 16,916 tags with more than 2 hits were selected to avoid the effect of sequencing errors in the libraries. From these candidate genes, 9614 nonredundant clones were obtained from Incyte Genomics (Incyte Corp., Beverly, MA), Clontech (Nippon Becton Dickinson, Tokyo, Japan), and Invitrogen (Invitrogen Japan K.K., Tokyo, Japan). Each clone was sequence validated and PCR amplified by Dragon Genomics (Takara Bio, Otsu, Japan), and the cDNA microarray slides (Liver chip 10k) were constructed using SPBIO 2000 (Hitachi Software, Fukuoka, Japan) as previously described.[13,15-19]

Laser Capture Microdissection. Hepatocytes in liver lobules and infiltrated lymphoid cells in the portal area were isolated by LCM using a CRI-337 LCM system (Cell Robotics, Albuquerque, NM)[18] (Fig. 1). Frozen liver biopsy specimens in OCT compound were sliced into sections 8 μm thick, immediately fixed in methanol for 5 minutes, and kept on dry ice. Tissue samples were quickly stained with toluidine blue and dissected. Around 500 lymphoid cells and a similar number of hepatocytes were excised from 3 slides and immersed in a denaturing solution. Dissection was completed within 5 minutes for each slide.

RNA Isolation and Antisense RNA Amplification. Total RNA was isolated from liver biopsy samples using an RNA extraction kit (Micro RNA Extraction Kit, Stratagene, La Jolla, CA). Aliquots of total RNA (5 μg) were subjected to amplification with antisense RNA (aRNA) using a Message Amp aRNA kit (Ambion, Austin, TX) as recommended by the manufacturer. About 25 μg of aRNA was amplified from 5 μg of total RNA, assuming that 500-fold amplification of mRNA was obtained. Total RNA from LCM samples was isolated with a carrier nucleic acid (20 ng poly C) using RNAqueous-Micro (Ambion). The quality and degradation of the isolated RNA were estimated after electrophoresis using an Agilent 2001 bioanalyzer (Agilent Technologies, Palo Alto, CA) (Fig. 1B). RNA isolation typically yielded 20-40 ng total RNA from 500 cells. Half of the obtained RNA was amplified twice as described above to yield 20-40 μg aRNA. Antisense RNA (20 μg) was used for further labeling procedures. The optimum conditions of LCM and reproducibility of data were assessed repeatedly.

Hybridization on cDNA Microarray Slides and Image Analysis. As a reference for each microarray analysis, aRNA samples prepared from the normal liver tissue from 1 of the patients were used. Test RNA samples fluorescently labeled with cyanine 5 (Cy5) and reference RNA labeled with Cy3 were used for microarray hybridization as described.[13,15-19] Quantitative assessment of the signals on the slides was carried out by scanning on a ScanArray 5000 (General Scanning, Watertown, MA) followed by image analysis using GenePix Pro 4.1 (Axon Instruments, Union City, CA) as described.

Processing of cDNA Microarray Data. Hierarchical clustering of gene expression was performed by BRB-Ar-

Table 1. Characteristics of Patients, as Used for Analyses of Whole Liver Biopsy, LCM, and SAGE Samples

Patient No.	Virus	Age	Sex	ALT	A	F	Viral load (LEG/mL, KIU/mL)	HCV serotype	HBeAg	LCM Hep	LCM Ly
Whole liver biopsy samples											
1	HBV	34	F	45	1	1	8.2	na.	+		
2	HBV	64	F	119	1	1	>8.7	na.	+		
3	HBV	49	M	21	1	1	<3.7	na.	−		
4	HBV	29	M	194	2	1	7.5	na.	+		
5	HBV	47	M	10	1	2	<3.7	na.	−		
6	HBV	53	F	43	1	2	7.3	na.	+		
7	HBV	24	M	42	2	2	7.1	na.	+		
8	HBV	18	M	400	2	2	8.0	na.	+		
9	HBV	20	M	188	2	2	6.2	na.	+		
10	HBV	59	M	68	2	3	4.4	na.	+		
11	HBV	36	F	29	2	3	4.2	na.	−		
12	HBV	60	M	33	2	3	7.4	na.	+		
13	HBV	60	F	28	2	3	<3.7	na.	−		
14	HBV	35	F	145	3	3	7.6	na.	+		
15	HBV	64	M	48	1	4	7.1	na.	−		
16	HBV	55	M	30	1	4	7.4	na.	−		
17	HBV	34	F	45	2	4	8.5	na.	+		
18	HBV	54	M	159	2	4	5.5	na.	+		
19	HBV	60	M	121	3	4	4.6	na.	+		
20	HCV	24	M	34	1	1	>850	I	−		
21	HCV	68	F	43	1	1	720	II	−		
22	HCV	64	F	117	1	2	590	na.	−		
23	HCV	69	M	6	1	2	300	II	−		
24	HCV	42	M	59	1	2	410	II	−		
25	HCV	73	M	19	1	2	140	I	−		
26	HCV	43	M	98	2	2	60	I	−		
27	HCV	70	M	56	2	2	600	I	−		
28	HCV	70	F	26	2	3	350	I	−		
29	HCV	65	M	21	2	3	290	I	−		
30	HCV	47	M	225	2	3	120	I	−		
31	HCV	58	M	200	2	3	410	I	−		
32	HCV	57	F	116	2	3	490	I	−		
33	HCV	63	F	39	2	4	290	I	−		
34	HCV	76	M	54	2	4	660	I	−		
35	HCV	67	M	67	2	4	240	I	−		
36	HCV	46	M	111	2	4	>850	I	−		
37	HCV	63	M	64	2	4	60	na.	−		
LCM samples											
38(2)	HBV	64	F	119	1	1	>8.7	na.	+	+	+
39	HBV	31	F	114	1	1	8.5	na.	+	+	+
40	HBV	68	F	41	2	2	5.5	na.	+		+
41	HBV	29	M	140	2	2	>8.7	na.	+		+
42	HBV	40	M	80	2	2	<3.7	na.	−		+
43	HBV	45	M	83	2	3	6.1	na.	+		+
44(10)	HBV	59	M	68	2	3	4.4	na.	+	+	+
45(14)	HBV	35	F	145	3	3	7.6	na.	+	+	+
46(21)	HCV	68	F	43	1	1	720	II	−	+	+
47	HCV	47	M	33	1	1	50	I	−	+	+
48	HCV	67	M	80	2	2	114	II	−		+
49	HCV	73	M	71	2	2	>850	II	−		+
50	HCV	67	M	70	2	2	>851	I	−		+
51	HCV	59	F	43	2	3	>852	I	−		+
52(31)	HCV	58	M	200	2	3	410	I	−	+	+
53(32)	HCV	57	F	116	2	3	490	I	−	+	+
SAGE samples											
54	HBV	55	M	34	1	1	5.9	na.	−		
55	HBV	70	F	31	2	2	7.7	na.	−		
56	HBV	72	M	22	1	4	6.3	na.	+		
57	HCV	71	M	128	1	4	440	I	−		
58	HCV	69	F	84	2	4	212	I	−		
59	HCV	49	M	150	2	4	60	I	−		

Abbreviations: na., not applicable; LCM, laser capture microdissection; ALT, alanine aminotransferase; SAGE, serial analysis of gene expression; A, activity; Hep., hepatocyte obtained by LCM; Ly., lymphocyte obtained by LCM; F, fibrosis; No., if the sample was obtained from the same patient, the new sample number is shown with the old one; HCV RNA was assayed by Amplicor Monitor Test (KIU/mL); HBV DNA was assayed by transcription-mediated amplification (LEG/mL).

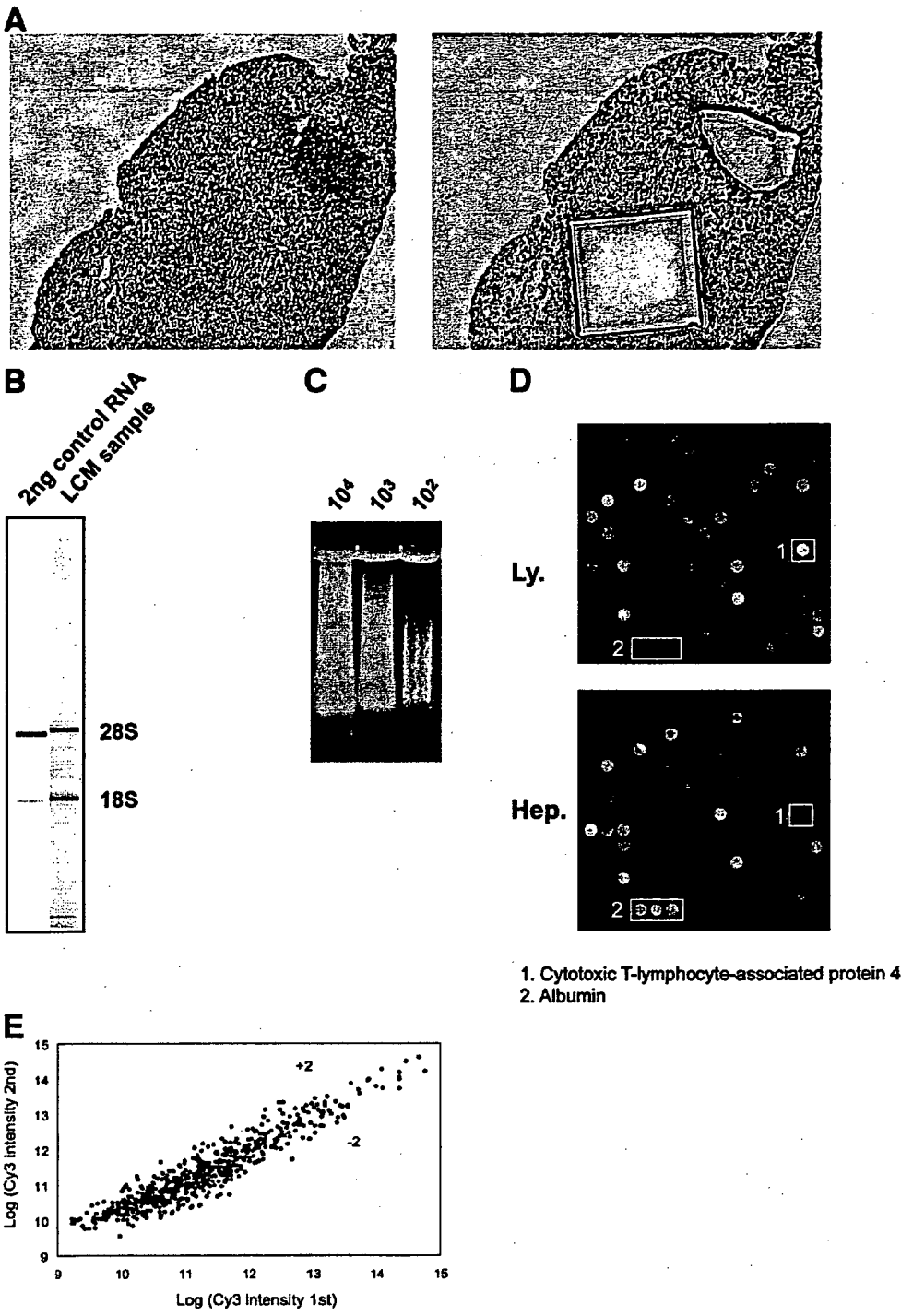

Fig. 1. Optimization of LCM and cDNA microarray analysis. (A) Toluidine blue staining of liver biopsy specimens before (left) and after (right) LCM. (B) Electrophoresis of isolated RNA using an Agilent 2001 bioanalyzer. (C) Two round-amplified aRNA from 10^2-10^4 excised hepatocytes. (D) Typical hybridization result from LCM samples. (E) Correlation of signal intensity between first and second amplified genes. Two values were significantly correlated ($P < .001$, $r^2 = .97$) within 2-fold differences.

rayTools (http://linus.nci.nih.gov/BRB-ArrayTools.htm). The filtered data were log-transferred, normalized, centered, and applied to the average linkage clustering with centered correlation. A class prediction was performed by compound covariate predictor incorporating genes that were differentially expressed at the $P = .002$ significance

Table 2. Supervised Learning Methods to Differentiate CHB and CHC

Classifier Category	Clinical Groups	Total Number of Cases	Number of Cases Misclassified	Classifier *P* Values	Number of Genes in the Classifiers ($P < .002$)
HBV versus HCV	HBV	19	1	<0.001	160
	HCV	18	3		
Histological stage	F1F2	17	10	0.402	55
	F3F4	20	7		
Histological activity	A0A1	13	6	0.173	106
	A2A3	24	6		
Age	≥50	22	9	0.298	39
	<50	15	6		
ALT at biopsy	≥80	14	7	0.200	21
	<80	23	6		

level as assessed by the random variance t test (BRB-ArrayTools). The univariate t test values for comparing the classes were used as the weights. The cross-validated misclassification rate was computed and at least 2,000 permutations were performed for a valid permutation P value. The Fisher and Kolmogorov-Smirnov tests were performed for gene ontology (GO) comparison ($P < .005$) (BRB-ArrayTools).

Pathway Analysis of Expression Data. The pathway analysis of the differentially expressed genes was performed using MetaCore software suite (GeneGo, St. Joseph, MI). Possible networks were created according to the list of the differentially expressed genes using the MetaCore database, a unique, curated database of human protein-protein and protein-DNA interactions; transcription factors; and signaling, metabolic, and bioactive molecules. The P value was calculated as:

$$p\text{-Value} = \frac{R!n!(N-R)!(N-n)!}{N!} \sum_{i=\max(r,R+n-N)}^{\min(n,R)} \frac{1}{i!(R-i)!(n-i)!(N-R-n+i)!}$$

where N is total number of nodes in the MetaCore database, R the number of network objects corresponding to the genes list, n the total number of nodes in each small network generated from the genes list, and r the number of nodes with data in each small network generated from the genes list. Moreover, direct interactions among the differentially expressed genes were examined. Each connection represents a direct, experimentally confirmed, physical interaction.

SAGE. Total RNA isolated from each of 3 patients with CH-B or CH-C was mixed to 200 μg in total, and polyadenylated RNA was extracted using a FastTrac mRNA Purification Kit (Invitrogen). The SAGE protocol was as described.[20,21] SAGE libraries were sequenced at random using an ABI Prism 377 DNA Sequencer and BigDye Terminator Cycle Sequencing Kit (PE Applied Biosystems, Foster City, CA). Sequenced files were analyzed with the SAGE version 1.00 software.

Quantitative Real-time Detection PCR. We performed quantitative real-time detection PCR (RTD-PCR) using TaqMan Universal Master Mix (PE Applied Biosystems). Primer pairs and probes for MxA, IP10, IFI15, OAS2, GZMA, TP53, PDECGF, IFNG, DIABLO, FGFB, BGA2, CASP9, PEX5, ANGPT1, VEGF, and β-actin were obtained from TaqMan assay reagents library. Results were expressed as means ± SEM. Significance was tested by 1-way ANOVA with Bonferroni's methods and differences were considered statistically significant at $P < .05$.

Results

Optimization of LCM and cDNA Microarray Analysis. Before analysis of region-specific gene expression, the sensitivity and reliability of linear aRNA amplification was examined. The quality and degradation of the isolated RNA were estimated after electrophoresis using an Agilent 2001 bioanalyzer (Fig. 1B). We successfully amplified aRNA from 10^2-10^4 excised hepatocytes with 2 rounds of amplification (Fig. 1C). The estimated amount of isolated RNA from around 150 excised hepatocytes (Fig. 1A) was 5-10 ng, and 10-20 μg of aRNA was obtained by 2 rounds of amplification, assuming that a 25×10^4-fold amplification (500-fold by single amplification) was carried out. A typical hybridization result is shown in Fig. 1D. Cytotoxic T lymphocyte-associated protein 4

Fig. 2. (A) Hierarchical clustering analysis of gene expression in hepatocytes and liver-infiltrating lymphocytes. Hep, hepatocyte; Ly, lymphocyte; B, hepatitis B; C, hepatitis C. (B) Hierarchical clustering analysis of 1,360 filtered genes (we excluded genes with an expression level within 1.5-fold of median value in more than 80% of samples) demonstrated more clear clusters of CH-B and CH-C.

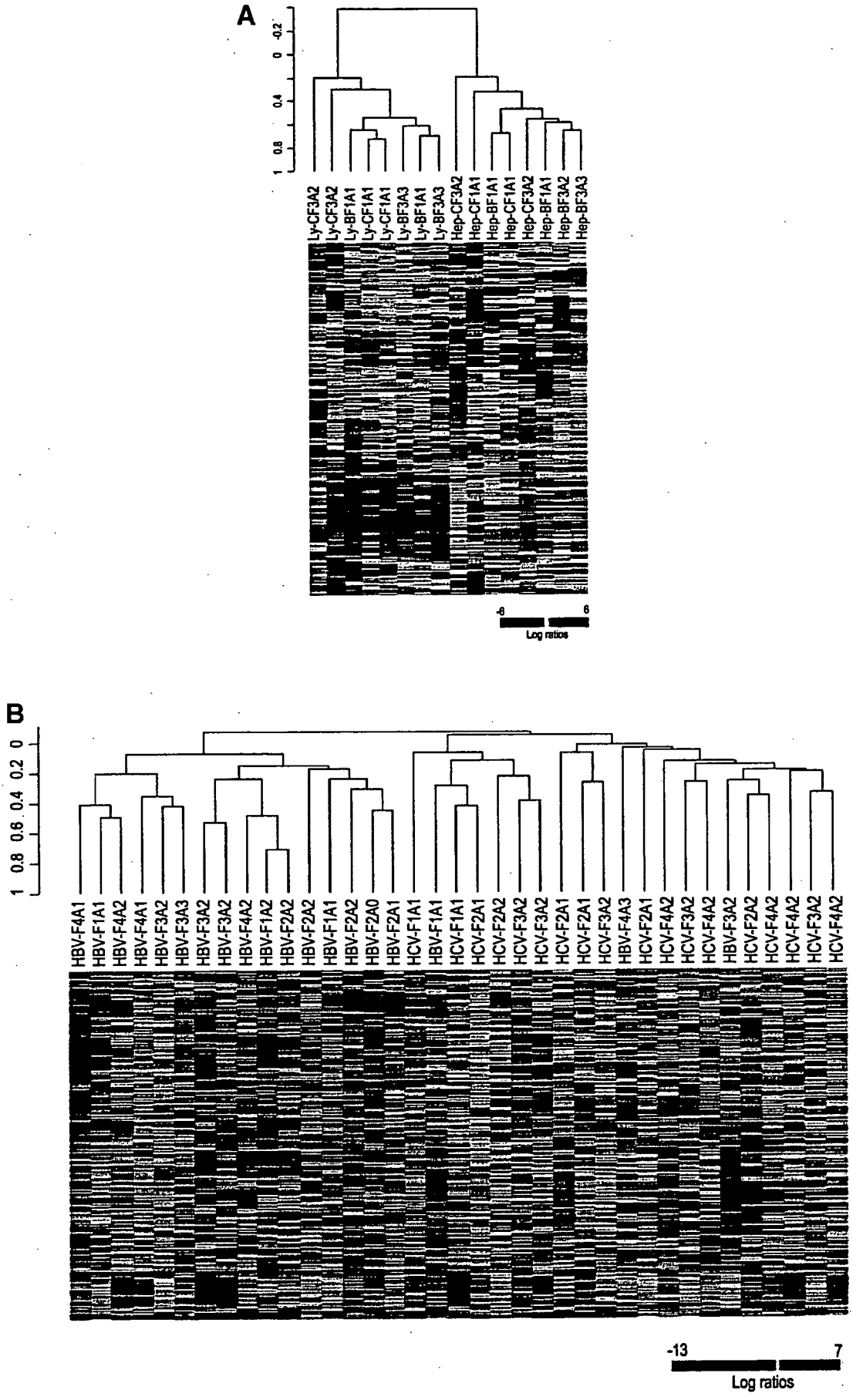
A
1 0.8 0.4 0 -0.2
Ly-CF3A2
Ly-CF3A2
Ly-BF1A1
Ly-CF1A1
Ly-CF1A1
Ly-BF3A3
Ly-BF1A1
Ly-BF3A3
Hep-CF3A2
Hep-CF1A1
Hep-BF1A1
Hep-CF1A1
Hep-CF3A2
Hep-BF1A1
Hep-BF3A2
Hep-BF3A3
-6
6
Log ratios
B
1 0.8 0.6 0.4 0.2 0
HBV-F4A1
HBV-F1A1
HBV-F4A2
HBV-F4A1
HBV-F3A2
HBV-F3A3
HBV-F3A2
HBV-F3A2
HBV-F4A2
HBV-F1A2
HBV-F2A2
HBV-F2A2
HBV-F1A1
HBV-F2A2
HBV-F2A0
HBV-F2A1
HCV-F1A1
HBV-F1A1
HCV-F1A1
HCV-F2A1
HCV-F2A2
HCV-F3A2
HCV-F3A2
HCV-F2A1
HCV-F2A1
HCV-F3A2
HBV-F4A3
HCV-F2A1
HCV-F4A2
HCV-F3A2
HCV-F4A2
HBV-F3A2
HCV-F2A2
HCV-F4A2
HCV-F4A2
HCV-F3A2
HCV-F4A2
-13
7
Log ratios

Fig. 2

was predominantly expressed in liver-infiltrating lymphocytes, whereas albumin was predominantly expressed in hepatocytes (Fig. 1D). To determine whether multiple amplifications affected the original gene expression, the signal intensities of first- and second-round amplified genes were compared. There was a significant correlation between the 2 values ($P < .001$, $r^2 = .97$), within a 2-fold difference (Fig. 1E), suggesting that the linear amplification procedure maintained the original level of gene expression.

Identification of Genes Differentially Expressed in Hepatocytes and Liver-Infiltrating Lymphocytes. Pairwise *t* test comparisons were applied and differentially expressed genes were identified in lymphocytes and hepatocytes in 4 patients with CH-B and 4 patients with CH-C (Supplementary Table 1-1). In hepatocytes, liver-specific proteins and enzymes such as fibrinogen, afamin, and cytochrome P450 were all expressed. In lymphocytes, cytokines, chemokines, and lymphocyte surface markers such as interleukin-7 receptor, chemokine (C-X-C motif) receptor 4, CD83 antigen, and CD69 antigen were all expressed (Supplementary Table 1-2). Hierarchical clustering analysis of gene expression in hepatocytes and liver-infiltrating lymphocytes demonstrated clear differences in gene expression (Fig. 2). Representative differentially expressed genes in lymphocytes and hepatocytes in CH-B and CH-C are summarized in Supplementary Tables 2-1, 2-2, 3-1, and 3-2.

Supervised and Nonsupervised Learning Methods to Classify Gene Expression Profiling According to Different Clinical Parameters. To examine which clinical parameters contributed to the changes in gene expression, supervised and nonsupervised learning methods were applied to classify gene expression profiles. The gene expression profiles of whole liver biopsy specimens, obtained from 19 patients with CH-B and 18 with CH-C, were analyzed. Hierarchical clustering analysis; a nonsupervised learning method, using 9641 nonfiltered genes, clearly demonstrated 2 clusters in CH-B and CH-C with a few exceptions (data not shown). Hierarchical clustering analysis with 1360 filtered genes (we excluded genes with an expression level within 1.5-fold of the median value in more than 80% of samples) demonstrated clearer clusters in CH-B and CH-C (Fig. 2B). Supervised learning methods based on the compound covariate predictor revealed that, among various clinical parameters including etiology (HBV or HCV), histological stage (F_1F_2 or F_3F_4), activity (A_0A_1 or A_2A_3), age ($\geq$50 or <50 years), and alanine aminotransferase (ALT) level at biopsy ($\geq$80 or <80 IU/mL), only etiology significantly classified these patients (Table 2). Thus, HBV or HCV infection determines gene expression to a greater degree than any other clinical parameters, such as histological stage and disease activity.

Differentially Expressed Genes in CH-B and CH-C Hepatic Lesions. The 160 genes were differentially expressed in CH-B and CH-C by class prediction analysis ($P < .005$); representative genes (greater than 3-fold difference in *t* value) are listed in Tables 3 and 4. Based on the expression profiles of hepatocytes and lymphocytes isolated using LCM, genes expressed in both hepatocytes and lymphocytes are described as Hep/Ly (Tables 3 and 4). Genes expressed at a significantly greater level in hepatocytes than lymphocytes were described as Hep. Genes expressed at a significantly greater level in lymphocytes than hepatocytes were described as Ly. In CH-B, genes involved in cell cycle arrest and induction of apoptosis were preferentially expressed. Several hepatocyte-specific and apoptosis-inducing genes such as Diablo homolog (cytochrome c/apaf-1/caspase-9 pathway activator) and BCL2-associated athanogene 2 (inhibitor of heat shock protein 70) were upregulated (Table 3, Fig. 7). In CH-C, cell cycle accelerating, immune-related, and antigen-presenting genes were preferentially upregulated. Many type 1 IFN-induced genes such as IFN-α-inducible protein 27 and IFN-α-inducible protein (clone IFI-15K) were upregulated in CH-C. The induction of these genes was confirmed by examining gene expression in Huh-7 cells treated with recombinant IFN-α (Tables 3 and 4, Fig. 7).

The frequent pathway processes observed in CH-B and CH-C using MetaCore are shown in Table 5. Induction of genes related to apoptosis (caspase activation via cytochrome C), transcription, and fibrosis (intermediate filament-based process and TGF-β receptor signaling pathway) were upregulated in CH-B, whereas genes related to immune reaction (defense response, antigen presentation, Golgi vesicle transport, and ubiquitin cycle), lipid metabolism (regulation of cholesterol absorption), and epidermal growth factor receptor (EGFR) signaling were upregulated in CH-C. This suggests that there are different signaling pathways in CH-B and CH-C.

Go Comparison of Expressed Genes in CH-B and CH-C Hepatic Lesions. The analysis of differentially expressed genes could underestimate the presence of mean full signaling pathways that were coordinately upregulated or downregulated, with subtle differences at an individual gene level. The biological significance of these coordinately regulated signaling pathways has recently been demonstrated.[22] Therefore, we applied the GO comparison tool to expressed genes in CH-B and CH-C hepatic lesions. The comparison tool provided a list of GO categories that were coordinately regulated between CH-B and CH-C.

Table 3. Differentially Upregulated Genes in Liver of Chronic Hepatitis B

Gene	GenBank ID	P Value	t Value HBV/HCV*	Hep/Ly	GO: Molecular Function
Viral genome					
HBV-core	X01587	0.000	6.69	Hep	Viral genome
Cell cycle and growth related					
V-ets erythroblastosis virus E26 oncogene homolog 2	NM_005239	0.001	3.97	Hep/Ly	skeletal development
RAP2A, member of RAS oncogene family	AI698376	0.000	3.91	Hep/Ly	signal transduction
Melanoma antigen, family C, 1	NM_005462	0.001	3.76	Hep/Ly	regulation of transcription
Cell division cycle 27	NM_001256	0.001	3.54	Hep/Ly	cell proliferation
Cyclin H	NM_001239	0.000	3.10	Hep/Ly	DNA repair
Immune response					
Interferon regulatory factor 6	NM_006147	0.000	3.80	Hep	regulation of transcription, DNA-dependent
Proteoglycan 2, bone marrow	R28336	0.001	3.65	Hep/Ly	defense response to bacteria
Chemokine (C-C motif) ligand 16	AW827147	0.001	3.49	Hep/Ly	chemokine activity
Janus kinase 2 (a protein tyrosine kinase)	NM_004972	0.001	3.48	Ly	JAK-STAT cascade
Chemokine (C-X-C motif) receptor 3	NM_001504	0.000	3.03	Hep/Ly	G-protein coupled receptor protein signaling pathway
Cell death					
BCL2-associated athanogene 2	NM_004282	0.000	3.95	Hep	apoptosis
Fas (TNFRSF6) associated factor 1	AA831837	0.001	3.74	Hep/Ly	apoptosis
Proline dehydrogenase (oxidase) 1	R88591	0.000	3.73	Hep/Ly	induction of apoptosis by oxidative stress
Caspase 9, apoptosis-related cysteine protease	NM_032996	0.001	3.58	Hep/Ly	apoptotic program
Purinergic receptor P2X, ligand-gated ion channel, 1	NM_002558	0.003	3.52	Hep/Ly	apoptosis
Tumor suppressing subtransferable candidate 1	NM_003310	0.002	3.35	Hep/Ly	apoptosis
Tumor necrosis factor (ligand) superfamily, member 11	NM_033012	0.002	3.25	Hep	cell differentiation
Diablo homolog (*Drosophila*)	NM_019887	0.004	3.04	Hep	apoptosis
Cell communication					
Nexilin (F actin binding protein)	NM_144573	0.000	4.15	Hep/Ly	unknown
Neurogranin (protein kinase C substrate, RC3)	NM_006176	0.000	4.09	Hep	signal transduction
Collagen, type XV, alpha 1	NM_001855	0.000	4.08	Hep/Ly	extracellular matrix
Chromogranin B (secretogranin 1)	NM_001819	0.001	3.47	Hep/Ly	hormone activity
Prostaglandin I2 (prostacyclin) receptor (IP)	NM_000960	0.001	3.42	Ly	G-protein signaling
Integral membrane protein 2C	NM_030926	0.002	3.36	Ly	integral to membrane
Sperm autoantigenic protein 17	NM_017425	0.002	3.26	Hep/Ly	cAMP-dependent protein kinase regulator activity
Talin 2	AF007154		3.18	Ly	cell adhesion
Cadherin 16, KSP-cadherin	AI241319	0.003	3.11	Hep	cell adhesion
Syntaxin binding protein 6 (amisyn)	AA281449	0.004	3.03	Ly	cell adhesion
Stress response					
RAD51-like 1 (*S. cerevisiae*)	NM_002877	0.000	3.78	Hep/Ly	DNA repair
Metallothionein 1X†	BC053882	0.001	3.44	Hep	electron transport
Siah-interacting protein	AA069322	0.002	3.08	Hep/Ly	ubiquitin cycle
Metallothionein 2A‡	NM_005953	0.004	3.03	Hep	copper ion homeostasis
F-box and leucine-rich repeat protein 2	NM_012157	0.000	3.01	Hep/Ly	ubiquitin cycle
Development					
Wolf-Hirschhorn syndrome candidate 1	NM_133335	0.001	4.51	Hep/Ly	morphogenesis
Homeo box B2	AI292043	0.001	3.87	Hep/Ly	development
Neurogenic differentiation 1	NM_002500	0.000	3.38	Hep/Ly	cell differentiation
Opiate receptor-like 1	NM_000913	0.004	3.29	Hep/Ly	G-protein coupled receptor protein signaling pathway
Wingless-type MMTV integration site family, member 2B	NM_024494	0.002	3.14	Hep/Ly	frizzled-2 signaling pathway
Cell motility					
Oligophrenin 1	R81942	0.001	3.80	Hep/Ly	rho GTPase activator activity
ATP-binding cassette, subfamily C, member 9	H16193	0.004	3.06	Hep	transporters
Transporter					
Sodium channel, voltage gated, type VIII, alpha	NM_014191	0.004	3.78	Hep/Ly	cation transport
Enzymes					
HMT1 hnRNP methyltransferase-like 6 (*S. cerevisiae*)	NM_018137	0.001	4.44	Hep/Ly	s-adenosylmethionine-dependent methyltransferase
Chymotrypsin-like	NM_001907	0.001	3.74	Hep/Ly	negative regulation of blood coagula
Aspartoacylase (aminocyclase) 3§	NM_080658	0.005	3.26	Hep/Ly	metabolism
Transcription and signal transduction					
Hepatocyte nuclear factor 4, gamma	AW273065	0.000	4.38	Hep/Ly	regulation of transcription
Nuclear receptor coactivator 6	NM_014071	0.000	3.98	Hep/Ly	DNA recombination
Protein kinase C, gamma	NM_002739	0.001	3.88	Hep/Ly	intracellular signaling cascade
T-box 2	NM_005994	0.000	3.82	Hep/Ly	development
Zinc finger protein 167	NM_018651	0.003	3.49	Hep/Ly	regulation of transcription, DNA-dependent
Small nuclear ribonucleoprotein polypeptide A	AI491862	0.002	3.37	Hep/Ly	intracellular signaling cascade
Zinc finger protein 266	NM_198058	0.002	3.03	Ly	regulation of transcription, DNA-dependent

*The univariate *t*-statistics for comparing the classes are used as the weights. †3.9-fold induction, ‡7.7-fold induction, and §1.8-fold induction by IFN-α in Huh-7 cells

In accordance with pathway analysis, antigen-presenting major histocompatibility complex molecules and IFN-α-induced genes were preferentially upregulated in CH-C (Table 6, Fig. 3). Genes related to apoptosis, DNA repair and cell death were upregulated in CH-B. DNA repair and apoptosis-related transcription factors were upregulated in CH-B, whereas anti-apoptosis and cell proliferation-related transcription factors were upregulated in CH-C. Platelet activating factor was upregulated in CH-C. As for metabolism-related gene regulation, peroxisome-associated genes were

Table 4. Differentially Upregulated Genes in Liver of Chronic Hepatitis C

Gene	GenBank ID	P Value	t Value HCV/HBV	Hep/Ly	IFN Induced	GO: biological process
Cell cycle and growth related						
Hect domain and RLD 5	NM_016323	0.000	4.50	Hep/Ly	7.7	regulation of cyclin dependent protein kinase activity
Inhibitor of growth family, member 4	NM_198287	0.001	3.50	Hep/Ly		grow arest
Phosphoinositide-3-kinase, class 3	AI446184	0.001	3.42	Hep/Ly		inositol or phosphatidylinositol kinase activity
Non-metastatic cells 1, protein (NM23A) expressed in	NM_000269	0.002	3.28	Hep		CTP biosynthesis
Mitogen-activated protein kinase kinase kinase 10	AI991621	0.003	3.23	Hep/Ly		JNK cascade
Immune responces						
Interferon, alpha-inducible protein 27	NM_005532	0.000	6.29	Hep	2.4	response to pest, pathogen or paras
Interferon, alpha-inducible protein (clone IFI-15K)	NM_005101	0.000	4.65	Hep/Ly	27.9	cell-cell signaling
Myxovirus (influenza virus) resistance 1	NM_002462	0.000	4.28	Hep/Ly	49.9	
Cold autoinflammatory syndrome 1	NM_183395	0.000	4.14	Ly		inflammatory response
Interferon-stimulated transcription factor 3, gamma 48kD	NM_006084	0.000	3.89	Hep/Ly	1.8	immune response
Beta-2-microglobulin	NM_004048	0.001	3.63	Hep/Ly	2.7	antigen presentation, endogenous antigen
2'-5'-oligoadenylate synthetase 2 (69-71 kD)	AA731148	0.001	3.49	Hep/Ly	3.3	immune response
Interferon-induced protein 44-like	NM_006820	0.001	3.42	Ly	4.5	immune response
Apolipoprotein L, 3	AW002766	0.003	3.23	Ly		inflammatory response
Immunoglobulin kappa constant	BC062732	0.004	3.04	Ly		immune response
Cell death						
Defender against cell death 1	NM_001344	0.000	4.11	Hep/Ly		apoptosis
HIV-1 Tat interactive protein 2, 30kDa	NM_006410	0.004	3.03	Hep/Ly		induction of apoptosis
Cell communication						
Major histocompatibility complex, class I, C	NM_002117	0.001	3.74	Hep/Ly		antigen presentation
CD97 antigen	NM_078481	0.001	3.72	Ly		cell adhesion
Major histocompatibility complex, class I, B	NM_005514	0.002	3.38	Hep/Ly	1.9	antigen presentation
Carcinoembryonic antigen-related cell adhesion molecule 5	NM_004363	0.002	3.30	Hep/Ly		integral to plasma membrane
Major histocompatibility complex, class II, DQ beta 1	NM_002123	0.002	3.25	Ly		antigen presentation
Major histocompatibility complex, class II, DR beta 4	NM_022555	0.002	3.25	Hep/Ly		antigen presentation
Dystroglycan 1 (dystrophin-associated glycoprotein 1)	AI684076	0.003	3.14	Hep/Ly		extracellular matrix
Dipeptidylpeptidase 6	NM_130797	0.004	3.11	Hep/Ly		integral to membrane
Ubiquitin and proteasome system						
Proteasome (prosome, macropain) subunit, beta type, 8	U17496	0.000	4.55	Hep/Ly		immune response
Ubiquitin D	NM_006398	0.003	3.13	Ly	2.1	antimicrobial humoral response
Proteasome (prosome, macropain) 26S subunit, non-ATPase, 2	NM_002808	0.004	3.05	Hep/Ly		regulation of cell cycle
Translation						
Eukaryotic translation elongation factor 1 beta 2	AI262506	0.000	4.46	Ly		protein biosynthesis
Eukaryotic translation initiation factor 1A, Y-linked	NM_004681	0.003	3.19	Hep/Ly	5.3	protein biosynthesis
Lipid metabolism						
Diacylglycerol O-acyltransferase homolog 1 (mouse)	NM_012079	0.002	3.31	Hep/Ly		O-acyltransferase activity
24-dehydrocholesterol reductase	NM_014762	0.003	3.19	Hep		cholesterol biosynthesis
Carnitine palmitoyltransferase II	NM_000098	0.005	3.01	Hep/Ly		fatty acid beta-oxidation
Nucleotide metabolism						
Adenosine deaminase, RNA-specific	NM_015841	0.001	3.46	Hep/Ly		RNA editing
Topoisomerase (DNA) I	J03250	0.003	3.22	Hep/Ly		DNA unwinding
THO complex 1	L36529	0.003	3.15	Hep/Ly		nuclear mRNA splicing, via spliceosome
Karyopherin alpha 3 (importin alpha 4)	NM_002267	0.003	3.14	Hep/Ly		NLS-bearing substrate-nucleus import
Nicotinamide nucleotide adenylyltransferase 1	NM_022787	0.004	3.06	Hep/Ly		NAD biosynthesis
Nuclear autoantigenic sperm protein (histone-binding)	M97856	0.005	3.00	Hep/Ly		DNA packaging
Ribonucleotide reductase M2 polypeptide	NM_001034	0.005	3.00	Ly		DNA replication
G protein binding protein						
Regulator of G-protein signalling 10	NM_002925	0.002	3.38	Hep/Ly		signal transduction
Transcription and signal transduction						
Staphylococcal nuclease domain containing 1	NM_014390	0.000	4.60	Hep/Ly		development
Ring-box 1	NM_014248	0.001	3.61	Ly		protein ubiquitination
Trophinin	NM_177558	0.001	3.44	Ly		embryo implantation
Forkhead box F1	AI453333	0.001	3.18	Hep/Ly	2.5	regulation of transcription, DNA-dependent
Nuclear antigen Sp100	M60618	0.003	3.02	Hep/Ly	5.8	regulation of transcription, DNA-dependent
Zinc finger protein 211	NM_198855	0.004	3.02	Ly		regulation of transcription, DNA-dependent
GA binding protein transcription factor, beta subunit 2, 47kDa	NM_181427	0.004	3.02	Hep/Ly		regulation of transcription, DNA-dependent
LIM protein (similar to rat protein kinase C-binding enigma)	AI445592	0.004	3.01	Hep/Ly		heart development
Hematopoietic cell-specific Lyn substrate 1	NM_005335	0.005	3.00	Ly		intracellular signaling cascade
ADP-ribosylation factor 5	M57567	0.005	3.00	Hep/Ly		intracellular protein transport

upregulated in CH-B, whereas cholesterol biosynthesis was upregulated in CH-C.

To investigate these findings in more detail, lymphocytes and hepatocytes were separately isolated by LCM and their gene expression was examined (Table 6, Fig. 4A, Fig. 7). Cyclophilin A and cyclophilin C, encoding peptidyl-prolyl cis-trans isomerases, were upregulated in CH-C. A recent report describes inhibition of HCV replication in Huh-7 cells by cyclophilin.[23,24] The upregulation of ssDNA-binding genes, such as p53 and RAD, and the relative downregulation of mitochondrial genes in hepatocytes, in CH-B, reflect a strong DNA damage response inducing apoptosis. Many IFN-α-induced genes were upregulated in hepatocytes rather than lymphocytes in CH-C.

CD4, CD8, linker for activation of T cells, and pro-apoptotic genes were upregulated in lymphocytes

Table 5. Pathway Analysis

Frequent Pathway Process	P Value
Whole liver tissue in CHB (n = 19)	
Caspase activation via cytochrome c	7.04E-11
Regulation of transcription, DNA-dependent	1.66E-12
Intermediate filament-based process	1.24E-07
Calcium ion transport	9.08E-08
Regulation of blood pressure	2.94E-07
Protein amino acid phosphorylation	4.04E-07
Regulation of angiogenesis	5.35E-09
TGF-beta receptor signaling pathway	8.08E-11
Whole liver tissue in CHC (n = 20)	
Defense response	3.27E-06
Antigen presentation, endogenous antigen	6.79E-06
Golgi vesicle transport	5.22E-07
Lipid catabolism	6.61E-06
Regulation of cell cycle	2.43E-08
Regulation of cholesterol absorption	1.02E-05
EGF receptor signaling pathway	1.59E-09
Ubiquitin cycle	4.71E-05

in CH-B. Despite the activated T cell responses in CH-B, chemokine expression was induced more in the lymphocytes in CH-C than lymphocytes in CH-B (Fig. 4A). To examine the functional role of liver-infiltrating lymphocytes further, LCM samples were also obtained from 4 more patients with CH-B and 4 with CH-C. Gene expression was compared for lymphocyte subsets (84 CD markers, including 26 T cell makers, 21 B cell markers, 16 myeloid cell markers, 11 NK cell markers, and 12 AD markers). Among these, many T cell markers and Th1 cytokines were significantly more upregulated in CH-B than in CH-C lymphocytes. Conversely, B cell marker, Th2 cytokines, and chemokines were preferentially induced in CH-C (Fig. 4B-C). The differences in immune reaction in CH-B and CH-C may be a reflection of their different pathogenesis.

Detailed Gene Network Analysis of Differentially Expressed Genes in CH-B and CH-C. To obtain a detailed and comprehensive gene network underlying CH-B and CH-C, SAGE data were integrated with those from cDNA microarray analysis. We applied 361 upregulated genes in CH-B ($P < .05$) and 344 in CH-C ($P < .05$), obtained from cDNA microarray analysis, and 1924 upregulated genes in CH-B (more than 5-fold tag count differences) and 1780 in CH-C, obtained from SAGE analysis, to the construction of the knowledge-based gene network. To find the gene network among these induced genes, published results of interaction of individual genes were integrated with these results using MetaCore software. Direct interactions between individual genes were searched for. The gene network of these differentially expressed genes formed a complex interaction of individual genes; however, representative signaling pathways underlying CH-B or CH-C were identified (Fig. 5).

In CH-B, p53 and 14-3-3 interacting genes might play an important role in the induced signaling pathways. Transcriptional factors such as CCAAT/enhancer binding protein (C/EBP), c-JUN, and cAMP-responsive element binding protein 1 (CREB1) are possibly also important molecules regulating these signaling pathways. These molecules induced apoptosis and activated transcription and oncogenes. Such activation might activate

Table 6. Gene Ontology Comparison

GO Description	Number of Genes	LS Permutation (P Value)	KS Permutation (P Value)	HBV	HCV	Reference
Whole liver tissue						
Antigen presenting	15	0.00105	0.034	1.01	1.49	0.81
IFN-alpha induced	71	$<1 \times 10^{-5}$	0.000	1.49	2.09	1.16
Cell death	34	0.005	0.019	1.35	1.15	0.99
DNA repair	62	0.005	0.041	1.51	1.10	1.11
G_1/S transition of mitotic cell cycle	18	0.001	0.009	1.25	1.41	1.23
Transcription factor binding	74	0.017	0.001	1.33	1.33	1.30
Cholesterol biosynthesis	12	0.029	0.002	1.11	1.44	1.30
PDGF	22	0.005	0.012	1.08	1.33	1.13
Peroxisome	19	0.026	0.005	1.46	1.17	0.93
Hepatocytes						
Peptidyl-prolyl cis-trans isomerase activity	9	0.002	0.001	1.31	1.48	1.15
Single-stranded DNA binding	16	0.019	0.003	1.85	1.34	1.27
Mitochondria	110	0.005	0.010	0.89	1.52	1.14
IFN-alpha induced	77	0.004	0.146	1.62	5.77	1.35
Lymphocytes						
Immunological synapse	12	0.002	0.003	6.38	3.78	3.31
Induction of apoptosis via deathdomain receptors	7	0.004	0.018	1.53	1.02	1.07
Chemotaxis	54	0.004	0.069	1.35	1.78	1.14

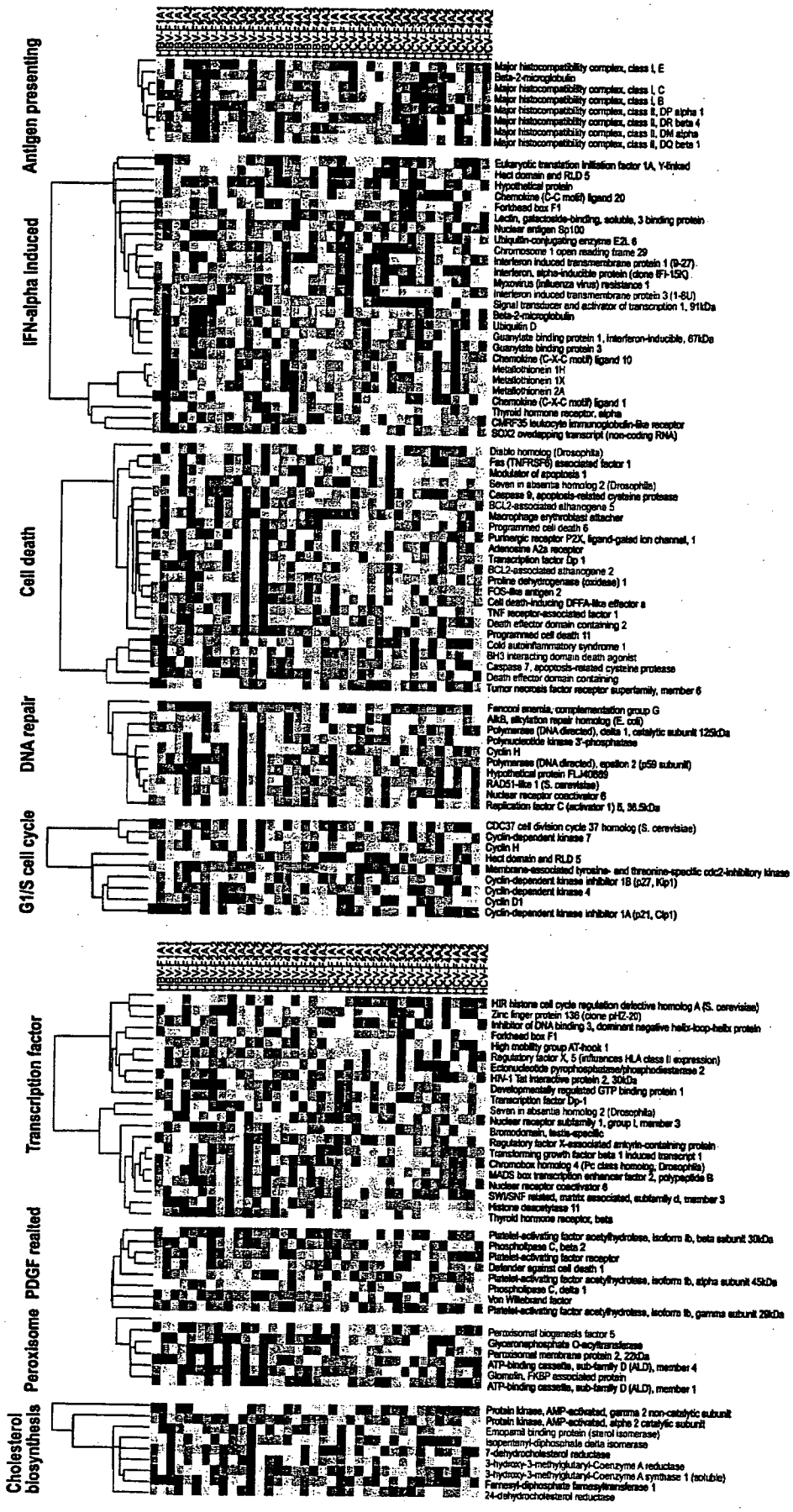

Fig. 3. One-way hierarchical clustering of whole liver samples with representative genes ($P < .05$) included in each GO category which was significantly different in CH-B and CH-C ($P < .005$). Green text denotes genes expressed predominantly in hepatocytes, and blue text denotes genes expressed predominantly in lymphocytes.

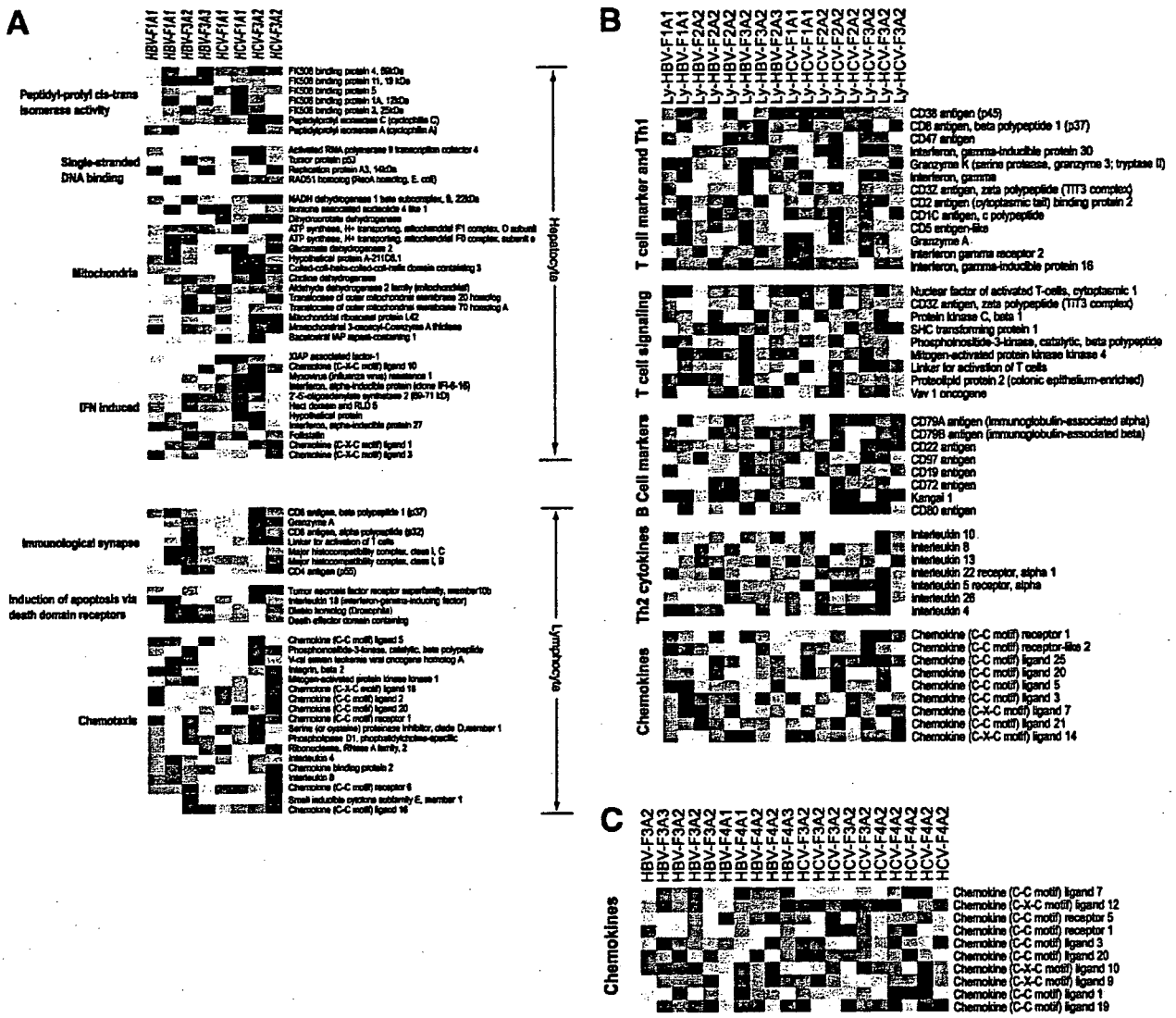

Fig. 4. (A) One-way hierarchical clustering of LCM samples with representative genes ($P < .05$). (B) One-way hierarchical clustering of liver-infiltrating lymphocytes, featuring specific gene sets of immune function. (c) One-way hierarchical clustering of whole liver sample gene sets of chemokines.

peroxisomes in CH-B (Fig. 5). In CH-C, type 1-IFN signaling (ISGF3/STAT1) might play a major role in the induced signaling pathways. The activation of the NF-κB and epidermal growth factor receptor (EGFR) signaling pathways may reflect liver inflammation and regeneration. These activations could lead to activation of liver X receptor/retinoid X receptor (LXR/RXR), a regulator of lipid metabolism.

Based on the database of MetaCore, which covers the entire regulation of the transcriptional factors, transcriptional regulation of differentially expressed genes was analyzed (Table 7). Transcription of mothers against decapentaplegic homolog 3 (SMAD 3), activator protein-1 (AP-1), p53, CREB1, and sterol regulatory element binding transcription factor 1 (SREB-1) was induced in CH-B, whereas NF-κB, IRF-1, STAT1, and retinoid acid receptor-alpha (RARα) signaling pathways were induced in CH-C. These differences fundamentally explain the different signaling pathways in CH-B and CH-C.

To examine whether these differences in gene expression contribute the different mechanism of hepatocarcinogenesis, we compared the angiogenic factors in CH-B and CH-C. The hierarchical clustering of patients using 34 angiogenesis-related genes obtained from cDNA microarray analysis, significantly clustered patients into 2 groups of CH-B or CH-C ($P = .0001$) (Fig. 6A). In CH-B, VEGF-family genes, FGF, and the angiopoietin

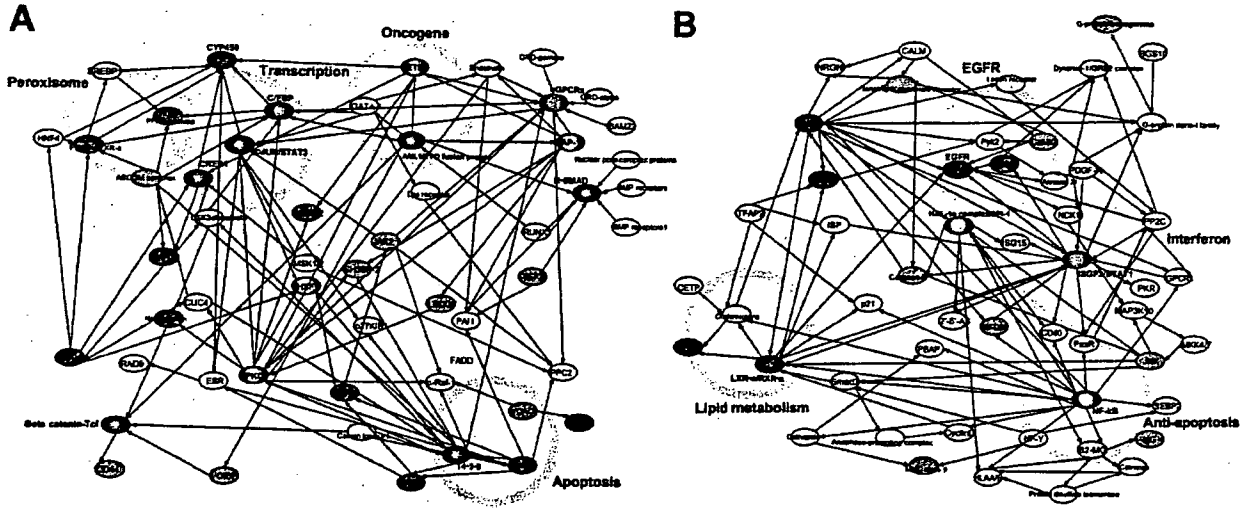

Fig. 5. (A) Gene network of differentially expressed genes in CH-B. (B) Gene network of differentially expressed genes in CH-C. Core transcription factors are represented by black ovals. Green ovals show genes expressed predominantly in hepatocytes and blue ovals show genes expressed predominantly in lymphocytes.

family were induced by several transcriptional factors including AP-1, c-fos, and STAT3, which were all strongly upregulated. In CH-C, inflammation-related angiogenic factors such as IL-8, IL-18, and PDGF1, induced by NF-κB, were also upregulated (Fig. 6B, Fig. 7). Thus, CH-B and CH-C showed different angiogenic properties, which implied that the tumorigenic process in CH-B and CH-C may differ.

Table 7. Transcription Regulation

	Frequent pathway process	P value
	Chronic hepatitis B	
1	Mothers against decapentaplegic homolog 3 (SMAD3)	5.25E-36
2	Activator protein-1 (AP-1)	4.24E-33
3	p53	8.49E-33
4	cAMP-responsive element binding protein 1 (CREB1)	2.39E-32
5	v-ets erythroblastosis virus E26 oncogene homolog 1 (ETS1)	3.38E-32
6	Sterol regulatory element binding transcription factor 1 (SREBP1)	6.73E-32
7	Transcription factor binding to IGHM enhancer 3 (TFE3)	9.48E-32
8	Signal transducer and activator of transcription 3 (STAT3)	1.33E-31
9	v-ets erythroblastosis virus E26 oncogene homolog 2 (ETS2)	1.88E-31
10	Transcription factor 7/Lymphoid enhancer binding factor 1 [Tcf(ref)]	1.88E-31
	Chronic hepatitis C	
1	Nuclear factor of κ light polypeptide gene enhancer in B-cells 1 (NF-κB)	1.32E-35
2	Interferon regulatory factor 1 (IRF1)	4.34E-33
3	Splicing factor 1(SF1)	9.17E-33
4	Signal transducer and activator of transcription 1 (STAT1)	1.28E-32
5	Retinoid acid receptor- (RAR)	1.81E-32
6	Nuclear factor of κ light polypeptide gene enhancer in B-cells 2 (RelA)	3.56E-32
7	Vitamin D receptor (VDR)	5.00E-32
8	Wilms tumor 1(WT1)	7.02E-32
9	Sterol regulatory element binding transcription factor 2 (SREBP2)	9.84E-32
10	Epidermal growth factor receptor (EGFR)	1.92E-31

Quantitative RTD-PCR. We performed quantitative real-time detection PCR (RTD-PCR) using 15 Taq-Man probes. The results of RTD-PCR on whole liver biopsy and LCM samples are shown in Fig. 7. In CH-B, apoptosis-inducing genes such as CASP9, IFNG, GZMA, TP53, BGA2, and DIABLO were upregulated. In CH-C, IFN-α-induced genes and chemokines such as MxA, IFI15, OAS2, and IP10 were upregulated. Angiogenic factors such as FGFB, ANGPT1, and VEGF were upregulated in CH-B, and another angiogenic factor, PDECGF, was upregulated in CH-C. The results are consistent with those from the cDNA microarray.

Discussion

The biological activity of viral coding polyproteins of HBV and HCV has been extensively investigated in cell lines and in transgenic mouse models. For example, accumulated evidence shows HBV-X protein to be a transcriptional transactivator that interacts with p53 tumor suppressor protein, modulating its signaling pathway.[9,25] The transgenic mouse model with overexpression of HCV polyproteins in the liver develops steatosis and HCC.[26,27] However, these findings have not been well evaluated in clinical samples.

Using in-house cDNA microarray analysis of 1080 genes, we previously reported differing gene expression profiles of liver tissue from patients with CH-B and CH-C.[13] However, the detailed signaling pathways underlying these diseases needed further clarification. In this study,

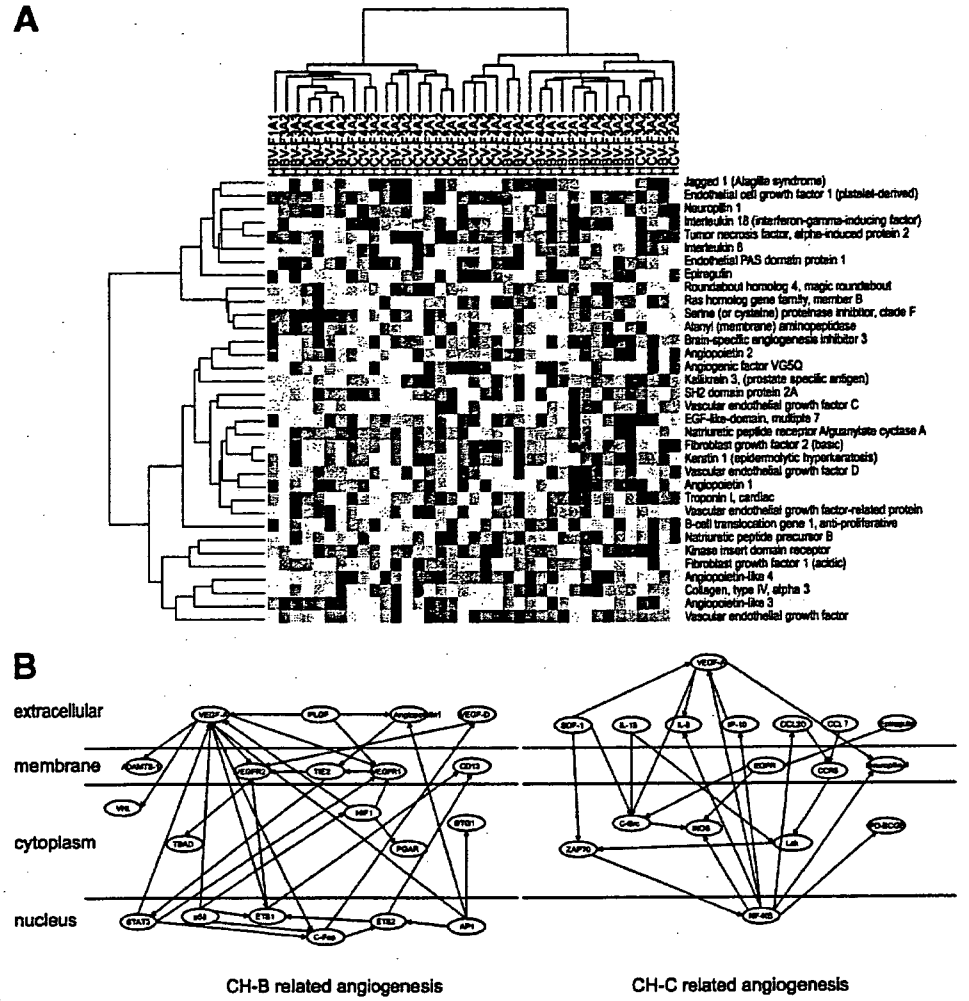

Fig. 6. (A) Hierarchical clustering of whole liver samples using angiogenic genes. (B) Gene network of angiogenic genes in CH-B and CH-C.

we constructed a new microarray slide, liver chip 10 K, consisting of 9614 clones which were selected from unique tag sequences in our hepatic SAGE libraries, including 667,067 tag sequences (manuscript in preparation), for the purpose of analyzing gene expression profiling in liver disease. We analyzed the gene expression profiles of whole liver biopsy specimens obtained from 37 patients with CH-B and CH-C. In addition, we selectively isolated liver-infiltrating lymphocytes (16 samples) and hepatocytes (8 samples) from liver biopsy specimens using LCM (Fig. 1D) and analyzed their gene expression. Furthermore, SAGE data were obtained from pooled samples of 3 CH-B or 3 CH-C patients, and their gene expression data were integrated to reveal the comprehensive, detailed gene network involved in CH-B and CH-C, respectively.

Hierarchical clustering analysis of 37 patients grouped these patients into 2 groups with CH-B or CH-C, with a few exceptions. Moreover, gene prediction analysis significantly discriminated between CH-B and CH-C patients ($P < .001$). HBV or HCV was the only factor significantly involved in patient classification, and other factors such as histological stage, disease activity, age, and ALT levels were not significantly associated with the classification of these patients. This indicates that virus type, whether HBV or HCV, influences liver gene expression to a greater degree than any other clinical parameter, such as degree of fibrosis or inflammation (Table 2).

The pathway analysis and GO comparison in CH-B and CH-C using whole liver biopsy revealed that antigen-presenting genes, IFN-α-induced genes, G_1/S transition genes, and cholesterol biosynthesis and platelet-derived factors were upregulated in CH-C, whereas genes related to cell death, DNA repair, and peroxisomes were upregulated in CH-B (Tables 5-6, Fig. 3). The association of HCV infection with steatosis in the liver in CH-C has

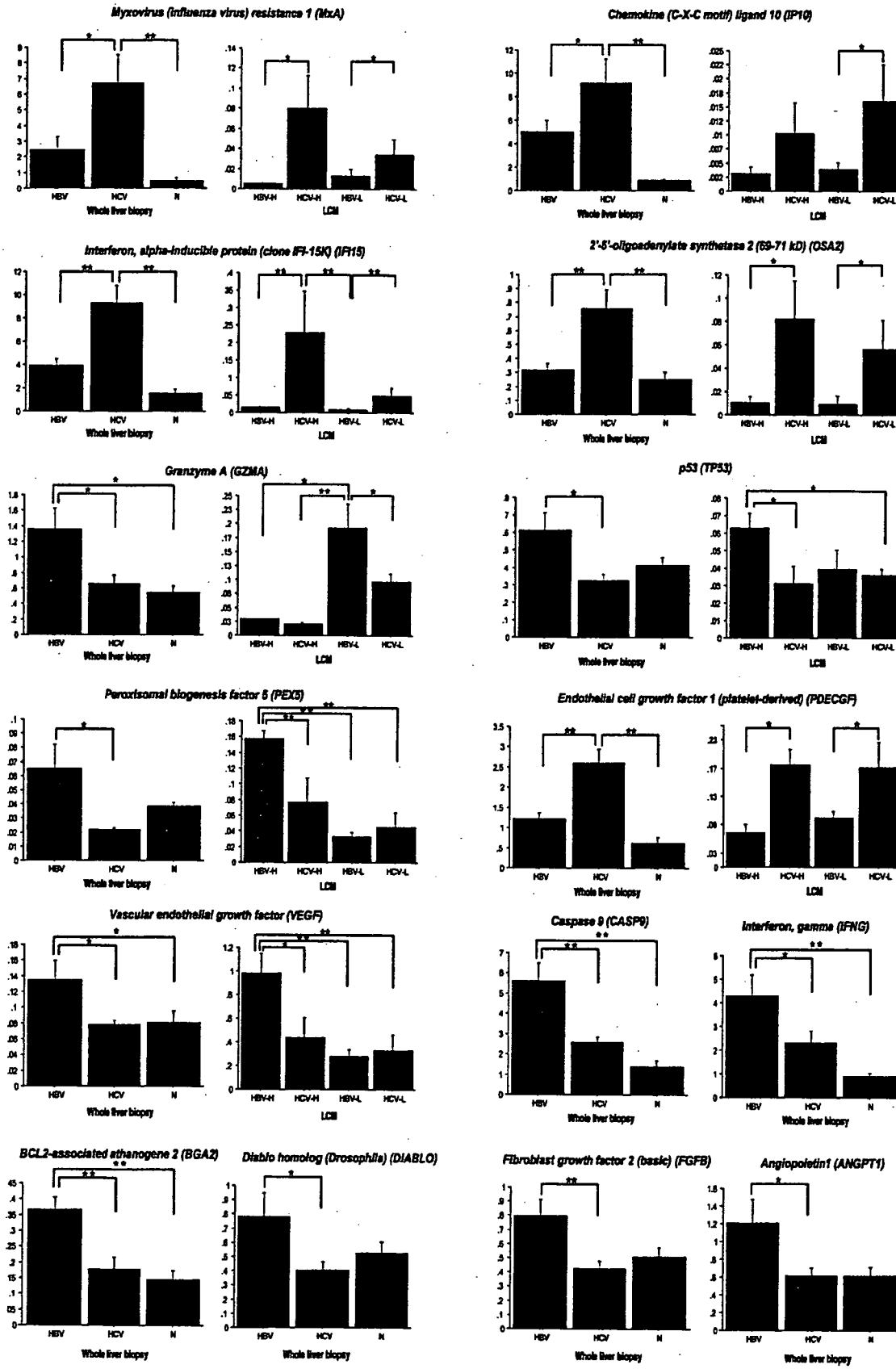

Fig. 7. Quantitative real-time detection PCR (RTD-PCR) using 15 TaqMan probes. The results of whole liver biopsy (HBV; 19 samples of CH-B, HCV; 18 samples of CH-C and N; 6 samples of normal liver) and LCM samples (HBV-H; 4 samples of hepatocyte in CH-B, HCV-H; 4 samples of hepatocyte in CH-C, HBV-Ly; 8 samples of lymphocyte in CH-B, HCV-Ly; 8 samples of lymphocyte in CH-C) were shown. $*P < .05$, $**P < .01$.

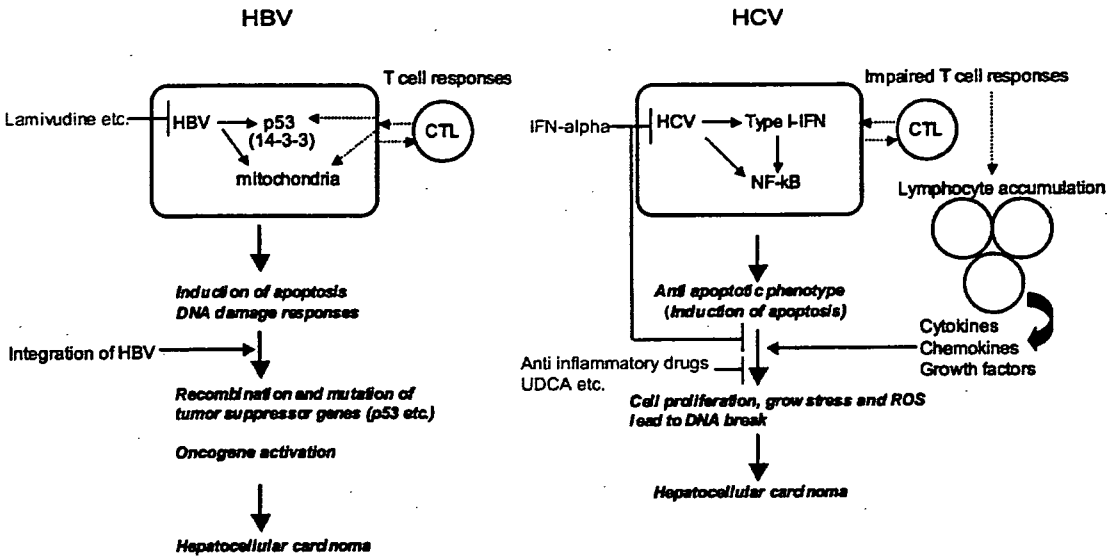

Fig. 8. Schematic representation of different pathogenesis of hepatitis and development of HCC in CH-B and CH-C.

been reported.[28,29] There might also be an association between HBV replication and peroxisomal activation, as reported using hepatoma-derived cell lines.[30,31] We combined SAGE data with those from cDNA microarray analysis and constructed the detailed and comprehensive gene network underlying CH-B and CH-C. In CH-B, p53-mediated and 14-3-3-mediated pro-apoptotic signaling; transcription factors such as AP-1, C/EBP, c-JUN, and CREB1; and oncogenes and peroxisomes were activated (Fig. 5). In CH-C, type 1-IFN (ISGF3/STAT1), NF-κB, EGFR, and LXR/RXR signaling were activated.

Lesion-specific gene expression analysis by LCM revealed more precise differences in gene expression between CH-B and CH-C (Fig. 4, Fig. 7), although a larger number of samples will be needed to reach concrete conclusions. Interestingly, many IFN-α-induced genes were upregulated in hepatocytes, but not in lymphocytes, in CH-C. On the other hand, DNA repair genes such as p53 and RAD were induced in hepatocytes in CH-B. Detailed analysis of lymphocyte markers revealed Th1-dominant responses in the liver in CH-B and Th2-dominant responses in the liver in CH-C.

Despite greater lymphocyte infiltration and homing in the liver, a weak T cell response and no T cell accumulation were observed in CH-C.[32,33] These contributed to the induction of various chemokines, cytokines, and growth factors, which may lead to cell proliferation and angiogenesis in CH-C. Surprisingly, gene expression profiling of angiogenic factors revealed clear differences in CH-B and CH-C. Many of the chemokines involved in angiogenesis are independent of VEGF-mediated or angiopoietin-mediated signaling pathways.[34] These findings possibly reflect a different means of carcinogenesis of HCC in CH-B and CH-C (Fig. 6).

In summary, we investigated the detailed signaling pathways in CH-B and CH-C. Although our data reveal the different signaling pathways induced in CH-B and CH-C, the precise mechanisms underlining these differences must be proven experimentally in the future. Nevertheless, from the therapeutic point of view, these results might be indicative that antiviral agents will be most effective for CH-B whereas anti-inflammatory drugs, other than IFN, would be effective for CH-C, for the prevention of HCC (Fig. 8). Further studies are needed to elucidate these findings clinically and biologically.

Acknowledgment: We thank Masami Ueda and Mikiko Nakamura for excellent technical assistance.

References

1. Shafritz DA, Shouval D, Sherman HI, Hadziyannis SJ, Kew MC. Integration of hepatitis B virus DNA into the genome of liver cells in chronic liver disease and hepatocellular carcinoma. Studies in percutaneous liver biopsies and post-mortem tissue specimens. N Engl J Med 1981;305:1067-1073.
2. Choo QL, Kuo G, Weiner AJ, Overby LR, Bradley DW, Houghton M. Isolation of a cDNA clone derived from a blood-borne non-A, non-B viral hepatitis genome. Science 1989;244:359-362.
3. Kiyosawa K, Sodeyama T, Tanaka E, Gibo Y, Yoshizawa K, Nakano Y, et al. Interrelationship of blood transfusion, non-A, non-B hepatitis and hepatocellular carcinoma: analysis by detection of antibody to hepatitis C virus. HEPATOLOGY 1990;12:671-675.
4. Huang HP, Tsuei DJ, Wang KJ, Chen YL, Ni YH, Jeng YM, et al. Differential integration rates of hepatitis B virus DNA in the liver of children with chronic hepatitis B virus infection and hepatocellular carcinoma. J Gastroenterol Hepatol 2005;20:1206-1214.